Proceedings of the 2002 Advanced Vehicle Control Conference, Hiroshima, Japan, September 2002

# Control of a Hybrid Electric Truck Based on Driving Pattern Recognition

**Chan-Chiao Lin, Huei Peng**
**Department of Mechanical Engineering**
**University of Michigan**
**Ann Arbor, MI 48109-2121**

**Soonil Jeon, Jang Moo Lee**
**School of Mechanical & Aerospace Engineering**
**Seoul National University**
**Seoul 151-742, Korea**

2250 G.G. Brown
Ann Arbor, MI 48109-2125 USA
Phone : +(734) 936-0352
Fax : +(734) 764-4256
E-mail : hpeng@umich.edu

The design procedure of a multi-mode power management control strategy with driving pattern recognition is proposed. The design goal of the control strategy is to minimize fuel consumption and engine-out NOx and PM emissions on diversified driving schedules. Six representative driving patterns (RDP) are designed based on the driving characteristics to represent different driving scenarios. For each RDP, the Dynamic Programming (DP) technique is utilized to find the optimal control actions. The implementable, sub-optimal control algorithms are then extracted by analyzing the behavior of the DP control actions. The driving pattern recognition (DPR) method is subsequently used to classify the current driving pattern into one of the RDPs to select proper control algorithm. This "multi-mode" control scheme was tested on several driving cycles and found to work satisfactorily.

Keywords / Hybrid Electric Vehicles, Powertrain Control, Heavy Duty Vehicles, Driving Pattern Recognition

## 1. INTRODUCTION

Over the last several years, many efforts were initiated, aiming to duplicate the success of hybrid powertrain on passenger cars to light and heavy trucks. The 21st Century Truck program in the US, spearheaded by two government agencies, Department of Energy and Department of Defense, is one such example. It is widely believed that the 3-times fuel economy improvement demonstrated by several prototype hybrid passenger cars, produced by the PNGV program, will be an unrealistic goal for hybrid trucks, especially if engine-downsizing is not an option. The recent announcement of proposed Euro and US EPA emission rules makes it very clear that emission reduction should be weighed more heavily in the design of hybrid trucks. In other words, it is important to address both fuel economy and emissions performance when considering the sizing and control laws for hybrid trucks.

The baseline truck studied in this paper is a Class VI, 7.3L diesel engine truck (International Truck, 4700 series), mainly used for urban delivery tasks. The fuel economy optimization problem for this truck has been presented in a previous publication [1], in which a hybrid configuration of the truck with a smaller engine (5.5L) and a 49KW electric motor was developed, and a sub-optimal controller which considers only fuel consumption was designed and analyzed.

In this paper, a multi-mode control algorithm for the fuel economy and engine-out emission optimization of the same parallel hybrid truck is presented. First, the design procedure for constructing sub-optimal control schemes was developed for six representative driving patterns (RDP). These rule-based, sub-optimal control schemes were obtained by learning the behavior of the optimal control laws under each of these driving modes, which were numerically solved by using the Dynamic Programming technique. In other words, a systematic procedure was developed to obtain rule-based control algorithms that approach the performance of the theoretically optimal DP results. It was found that the optimal DP results can be approximated by parameters associated with a power-split ratio curve, which makes it very easy to extract sub-optimal control rules.

A real-time driving pattern recognition (DPR) algorithm is then developed to switch between these six rule-based control strategies, with the assumptions that (i) driving pattern does not change fast and thus historical pattern is likely to continue into the near future; and (ii) the sub-optimal control strategies are different enough that selecting a proper one among them will result in significant performance improvements [2].

The DPR algorithm is developed base on the idea that driving scenarios can be differentiated by objective measures such as average power, braking energy, and the ratio of stop time to total time. It is judged that these measures can be extracted accurately by using data over a historical window, for example, during the past 150 seconds. Two kinds of Representative Driving Patterns can be constructed for the development of the real-time DPR algorithm--imaginary RDP and partial driving cycles. The imaginary RDP maneuvers are used in this paper. The DPR algorithm was then trained to ensure a high success rate in correctly identifying the driving pattern. Finally, six driving cycles that the DPR algorithm has never experienced before, are used to assess the overall performance of the proposed control system.

## 2. MODE-SPECIFIC SUB-OPTIMAL CONTROL

The power management control problem of Hybrid Electric Vehicles (HEV) has been widely studied in recent years. It is known that the main control challenge for HEV is to determine the proper operation mode, and the split ratio between the two power sources and the gear-shifting schedule. However, control strategies based on engineering intuition or trial-and-error normally fail to achieve satisfactory improvement due to the complex nature of HEVs and multiple objectives (fuel and emissions). In this section, a design procedure based on Dynamic Programming for the design of a sub-optimal control strategy is described.

### 2.1 Dynamic Programming Based Optimization

The control of HEVs is formulated as an optimal control problem in the Dynamic Programming approach [1]. The goal is to find the control action of the hybrid powertrain to minimize a cost function, which consists of the weighted sum of fuel consumption and emissions for a given driving cycle.

$$J = \sum_{k=0}^{N-1} \left[ fuel(k) + \mu \cdot NOx(k) + \upsilon \cdot PM(k) \right] + \alpha (SOC(N) - SOC_f)^2 \quad (1)$$

where $N$ is the duration of the driving cycle, and $\mu$ and $\upsilon$ are the weighting factors on the instantaneous engine-out NOx and PM emissions. A terminal constraint on SOC is imposed to maintain the battery energy and make it easier to calculate the average fuel economy. $SOC_f$ is the desired SOC at the final time of the cycle, which is usually the initial SOC also.

During the optimization procedure, it is necessary to impose inequality constraints to ensure safe and smooth operation of the engine/battery/motor. In addition, the equality constraints on the wheel speed and torque are added to assure that the vehicle always meets the speed and load (torque) demands of the driving cycle at each sampling time.

A powerful algorithm to solve the above optimization problem is the Dynamic Programming (DP) technique. DP has the advantage of finding the true optimality within the accuracy of computational grids [3]. However, the computation efficiency of DP is low due to the "curse of dimensionality". Several techniques including model reduction, pre-computed look-up tables and vectorized operation are adopted to accelerate the computation speed [4], [5].

To study the trade-off between fuel economy and emissions, the weighting factors are varied:

$$\begin{aligned} &\mu \in \{0,5,10,20,40\} \\ &\upsilon \in \{0,100,200,400,600,800\} \end{aligned} \quad (2)$$

The case of $\mu = \upsilon = 0$ corresponds to the optimal fuel economy scenario. Selected optimization results are shown in [4]. It has been found significant reduction in NOx and PM emissions can be achieved at the price of a small increase in fuel consumption. Hence, the case $\mu = 40, \upsilon = 800$ is chosen to obtain optimal control actions over the UDDSHDV cycle, which achieves a reduction of NOx and PM by 17.3 % and 10.3% respectively, at a 3.67% increase on fuel economy compared to the $\mu = \upsilon = 0$ case. The fuel economy and emission results from DP are shown in Table 1. The "new control" results are from the sub-optimal algorithm to be described in the next sub-section.

Table 1: Results over the UDDSHDV cycle

| | FE (mi/gal) | NOx (g/mi) | PM (g/mi) | Performance Measure * |
|---|---|---|---|---|
| Baseline Control | 13.11 | 5.770 | 0.460 | 843.96 |
| New Control | 12.81 | 4.866 | 0.435 | 793.16 |
| DP ( $\mu = 40, \upsilon = 800$ ) | 13.24 | 4.642 | 0.399 | 739.56 |

* Performance Measure: $fuel + 40 \cdot NOx + 800 \cdot PM$ (g/mi)

### 2.2 Development of Sub-Optimal Rule-Based Control

Although the Dynamic Programming approach provides an optimal solution, the resulting control policy is not implementable under real driving conditions because it requires the knowledge of future speed and load profile. The results are, on the other hand, benchmark which other control strategies can be compared to and learn from. Therefore, the second part of the HEV control design procedure involves knowledge extraction from DP results to obtain implementable rule-based control algorithms. Overall, the behaviors to learn include the transmission gear-shift strategy, the power-split strategy, and the charge-sustaining strategy. Here we assume that the regenerative braking strategy is simple—use as much regenerative braking as possible, subject to the current/power limit of the generator/battery. The difference between the regenerative braking and demand power will be supplied by the friction brake. This simple regenerative braking strategy assumes that the vehicle handling stability is not an issue.

The gear-shift strategy was found to be crucial for the fuel economy of hybrid electric vehicles. From DP results, the gear operational points are plotted on the standard transmission shift-map (Fig. 1). It can be seen that the gear positions are separated into four regions and the boundary between adjacent regions represents optimal gear shifting thresholds. A new gear-shift map can be obtained after a hysteresis function is added to the shifting lines.

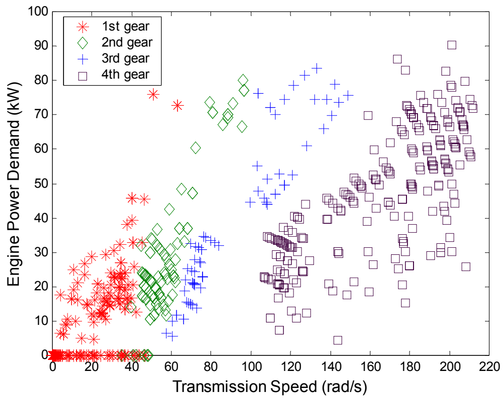


Fig. 1: Gear operating points of DP optimization

To identify the optimal power split of the hybrid powertrain, a power-split-ratio, $PSR = P_{eng} / P_{req}$ , is used to quantify the power flow action used by the DP algorithm. The optimal (DP) behavior was found to roughly follow a simple curve when we plot the optimal PSR versus the power request over the transmission input speed, which is equivalent to torque demand at the torque converter output shaft (see Fig. 2). This figure shows that the optimal policy uses the recharging mode ( $PSR > 1$ ) in the low torque region, the engine-only mode ( $PSR = 1$ ) in the middle torque region, and the power-assist mode ( $PSR < 1$ ) in the high torque region. A least-square curve fit is then used to approximate the optimal PSR, shown as the solid line in Fig. 2.

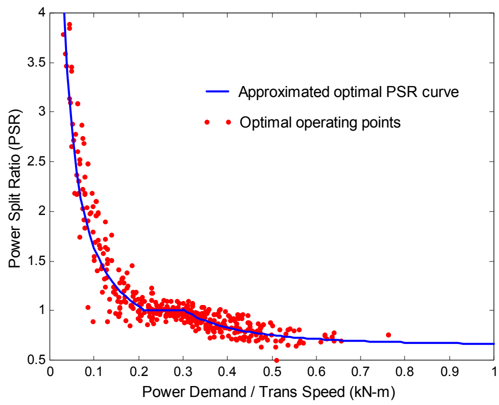


Fig.2: DP power split behavior (UDDSHDV cycle)

It should be noted that the power split control scheme described above can not assure the battery SOC will operate within a desired operating range. A charge-sustaining strategy should be developed to maintain the battery energy. More aggressive rules of spending battery energy can be used when SOC is high and more conservative rules can be used when SOC is low. These adaptive PSR rules can be learned from the DP policy by specifying different initial SOC points in the simulation.

The above new gear shifting control, power split control and charge-sustaining strategy are incorporated to construct the vehicle-level rule-based control strategy. This improved rule-based controller is evaluated using the original UDDSHDV cycle. A linear SOC correction procedure was used to calculate fuel economy and emissions [6]. The simulation results are shown in Table 1. It can be seen that the new rule-based control system improves the combined fuel and emission performance (the “performance measure”) over the original, intuition driven rule-based control law [4] and is slightly worse than the performance of the DP result which is optimal for the UDDSHDV cycle.

The improved rule-based control is learned from the optimization result over one specific driving cycle. It may not perform satisfactorily under other driving scenarios. This motivates the multi-mode control study to be presented in the next section.

## 3. DRIVING PATTERN RECOGNITION (DPR)

### 3.1 Multi-Mode Driving Control

The basic idea of multi-mode driving control based on DPR technique was addressed in a previous paper [2]. In a nutshell, this control concept assumes that we can use several Representative Driving Patterns (RDP) as basic templates, to represent all driving conditions. Switching among control rules optimized under each RDP is assumed to provide significant benefits. The switching will be determined by a DPR algorithm, which choose one of the RDP to approximate current driving situation. This overall control algorithm assumes the driving condition during a finite history window will likely to continue into the near future.

Fig. 3 shows the concept of the multi-mode driving control. It can be seen that the finite future control horizon ( $NT$ ) is much smaller than the final time ( $f T$ ) of each RDP. This characteristic is conceptually similar to that in the receding horizon control problem found in the optimal control literature. Here $T$ is the sampling time, and $pT$ is the size of history used to identify driving pattern by the DPR algorithm.

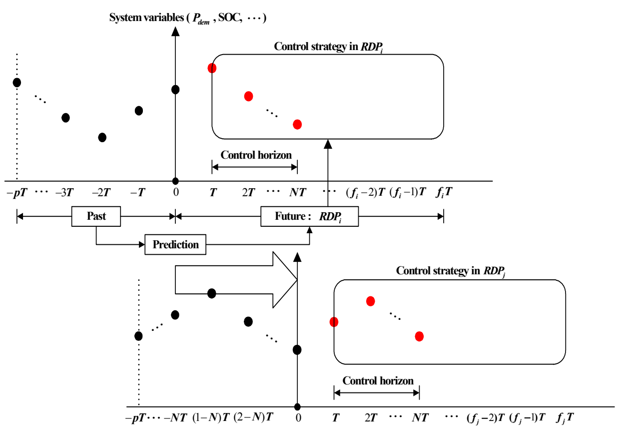


Fig. 3: Concept of multi-mode driving control based on DPR.

### 3.2 Characteristic Parameters for DPR

Four parameters characterize the power demand, and thus affect the strategy of HEV control: First, $P_{dem\_mean}$, the averaged positive power demand, which is related to the operating points of an engine and a motor during traction. The second parameter is $P_{dem\_std}$, the standard deviation of positive power demand during driving, which represents the variation of the positive power demand, which is influenced by both traffic condition and drivers' habit. The other two parameters are $P_{dem\_neg\_mean}$, averaged negative power demand and the ratio Stop time/Total time. These two parameters characterize whether the traffic is congested, and thus the amount of available regenerative braking, and fuel-cut off strategy.

Since the parallel HEV's control variables presented in Section 2 include power-split ratio between engine and motor, and sub-optimal gear ratio, we select the first two parameters ( $P_{dem\_mean}$ and $P_{dem\_std}$ ) as the main independent variables for DPR decisions. The correlation analysis among parameters shown in Fig. 4 and 5 supports this choice. These figures are obtained by simulating a hybrid passenger-vehicle over diverse driving cycles in ADVISOR [6]. Figures 4 and 5 show that there is strong correlation between the last two parameters and $P_{dem\_mean}$, i.e., it is possible to neglect the last two cycle parameters if $P_{dem\_mean}$ is properly used in the DPR algorithm.

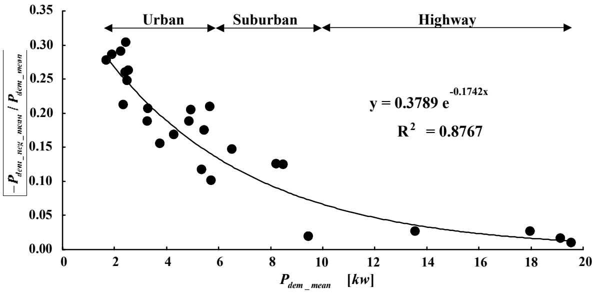


Fig. 4: Correlation between $P_{dem\_mean}$ and $-P_{den\_neg\_mean} / P_{dem\_mean}$

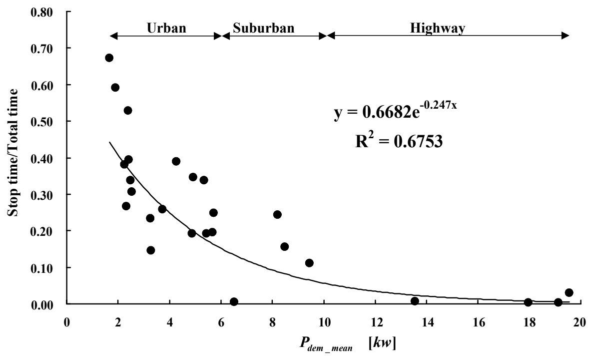


Fig. 5: Correlation between $P_{dem\_mean}$ and Stop time/Total time

### 3.3 Selection of Representative Driving Patterns (RDP)

Based on the two selected parameters for DPR, the next task is to choose RDP templates, which could be selected from defined driving cycles, or constructed from simple mathematical operations. We choose to go with the second approach, because of the fact the characteristic parameters can be easily scaled.

The flowchart and variables for defining imaginary RDPs with desired $P_{dem\_mean}$ and $P_{dem\_std}$ are explained in Fig. 6 and Table 2. The basic rules for this procedure are described below.

***Rule 1***: Once the desired $P_{dem\_mean\_des}$ and $P_{dem\_std\_des}$ are determined, the overall process for making imaginary RDP should proceed to achieve these desired $P_{dem\_mean\_des}$ and $P_{dem\_std\_des}$.

***Rule 2***: The sign of the power demand ( $P > 0$ or $P < 0$ ), is randomly selected. This randomness helps to ensure that the defined driving cycle is rich.

***Rule 3***: Once the sign of the power demand is selected, it will be used for a finite time $T_{\min\_pos}$ or $T_{\min\_neg}$ (sign-dependent). $T_{\min\_pos}$ is fixed at 4 seconds. $T_{\min\_neg}$ is randomly selected from four values: 2, 4, 6 , and 8 seconds.

***Rule 4***: The overall possible total power is divided into grid points. And the power to be used to calculate the next vehicle speed value is selected based on the values of $P_{dem\_mean\_des}$ and $P_{dem\_std\_des}$. For example, when $P > 0$, if $P_{14}$ is the grid point closest to $P_{dem\_mean\_des}$, and if $P_{dem\_std\_des}$ is small, one point in the Region 1 ( $P_{14}$ and its immediate two neighboring points) is randomly selected. If $P_{dem\_std\_des}$ is large, one point in the Region 2 ( $P_{14}$ and its immediate four neighboring points) is selected randomly.

***Rule 5***: When $P < 0$, one point is randomly chosen among all grid points.

Table 2: Variables used in the process to make imaginary RDPs.

| Variables | Explanations |
|---|---|
| $V$ | Vehicle velocity [*km/h*]<br>$V_0$ : Present value<br>$V_{11}, V_{12}, V_{13}, \cdots$ : Future candidates after $\Delta T$ ( $\Delta T = 1$ second) |
| $P$ | Power demand [*kw*]<br>$P_0$ : Power demand corresponding to $V_0$<br>$P_{11}, P_{12}, P_{13}, \cdots$ : Power demand corresponding to $V_{11}, V_{12}, V_{13}, \cdots$<br>( $P_{\min} = -30$ [*kw*]) |

| | |
|---|---|
| Simple shifting map | Gear 1 when $V < 15.0\,[km/h]$<br>Gear 2 when $15.0 \le V < 35.0\,[km/h]$<br>Gear 3 when $35.0 \le V < 50.0\,[km/h]$<br>Gear 4 when $V \ge 50.0\,[km/h]$ |

It is assumed that we only need to choose a small number of RDPs to train the DPR algorithm. The six RDPs created from the above process are summarized in Table 3. Fig. 7 and Fig. 8 show two of the extreme RDPS (low average, high standard deviation, and high average, low standard deviation).

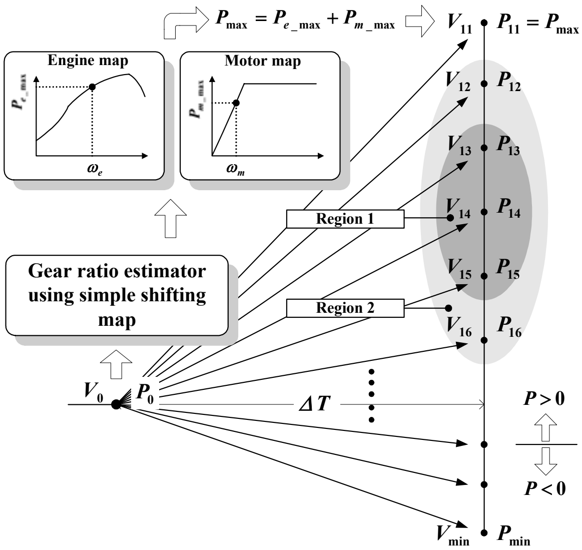

Fig. 6: Process for defining imaginary RDPs.

Table 3: Six imaginary RDPs.

| # of RDP | $P_{dem\_mean}\,[kw]$ | $P_{dem\_std}\,[kw]$ |
|---|---|---|
| 1 | 33.123 | 29.311 (H) |
| 2 | 32.353 | 12.087 (L) |
| 3 | 54.810 | 38.020 (H) |
| 4 | 49.544 | 21.102 (L) |
| 5 | 71.398 | 39.980 (H) |
| 6 | 70.164 | 26.740 (L) |

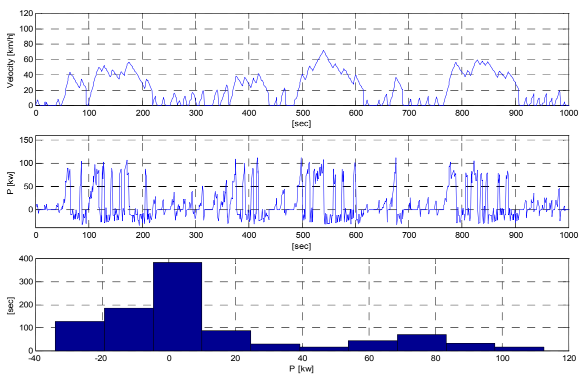
Fig. 7: RDP 1

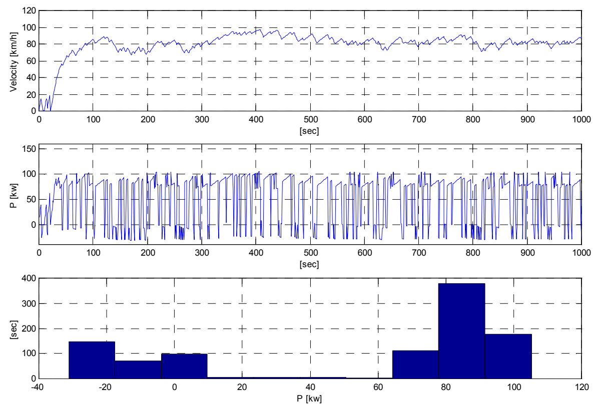
Fig. 8: RDP 6

## 4. SIMULATION RESULTS

For each Representative Driving Pattern, the sub-optimal control algorithm is derived from applying the design procedure illustrated in Section 2. Table 4 shows the simulation results when the sub-optimal control rule extracted over each RDP is applied to that corresponding RDP. $P_{ii}$ represents the HEV performance (weighted summation of fuel consumption and emissions) when the i-th sub-optimal control rule is used in the *i*-th RDP. Note that these values are idealized, trained data and do not represent real performance.

The concept of the multi-mode control strategy is illustrated in Fig. 9. First, the historical values of the driver power demand in the buffer with the size of $pT$ seconds are stored. Every $NT$ seconds, the DPR processor takes the stored power demand values to calculate the mean and standard deviation and then classify the current driving pattern into one of the six RDPs. The six sub-optimal control rules ($C_1$~$C_6$) are stored in the multi-mode control module for switching according to the DPR selection.

The effectiveness of the multi-mode control is verified through the simulations over driving cycles that have not been involved in the selection of RDPs or experienced by the DPR algorithm. The overall performance measure ( $FC + 40 \cdot NOx + 800 \cdot PM$ ) of the multi-mode control is compared with the one of the single-mode control which uses a sub-optimal control rule extracted only from the UDDSHDV cycle. Table 5 and Table 6 show the simulation results of the single-mode and multi-mode controller over six different cycles. The results for the UDDSHDV cycle are also included. For comparison purposes, the optimal performance achieved by the DP algorithm is also presented. For these simulations, the variables for multi-mode control ( $pT$ and $NT$ ) are 150 and 5 seconds, respectively. Compared to the single-mode control results, the multi-mode control has a better performance over most of the test cycles, a similar performance over WVUINTER cycle, yet a worse performance over UDDSHDV. Considering the fact the single-mode control rule is extracted from the UDDSHDV cycle, this is understandable. It is important to point out that the tuning of $pT$ and $NT$ is required to get the better results.

Table 4: HEV performance over each RDP.

| # of RDP | Sub-optimal control map | HEV performance $FC + 40 \cdot NOx + 800 \cdot PM$ [$g/mile$]. |
|---|---|---|
| 1 | $C_1$ | $P_{11} = 628.51$ |
| 2 | $C_2$ | $P_{22} = 407.91$ |
| 3 | $C_3$ | $P_{33} = 826.62$ |
| 4 | $C_4$ | $P_{44} = 666.51$ |
| 5 | $C_5$ | $P_{55} = 959.76$ |
| 6 | $C_6$ | $P_{66} = 999.12$ |

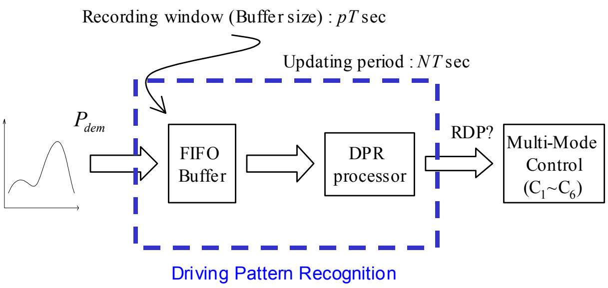


Fig. 9: Diagram of multi-mode control strategy

Table5: Simulation results of multi-mode control.
$fuel + 40 \cdot NOx + 800 \cdot PM$ [$g/mile$]

| | UDDSHDV | WVUCITY | WVUSUB | WVUINTER |
|---|---|---|---|---|
| Single-mode | 793.16 | 494.12 | 582.18 | 896.00 |
| Multi-mode | 801.64 | 468.38 | 576.39 | 897.22 |
| DP | 739.56 | 403.58 | 526.67 | 847.67 |

Table 6: Simulation results of multi-mode control.
$fuel + 40 \cdot NOx + 800 \cdot PM$ [$g/mile$]

| | NYCCOMP | NYCTRUCK | Manhattan |
|---|---|---|---|
| Single-mode | 401.17 | 667.70 | 786.74 |
| Multi-mode | 381.89 | 659.63 | 771.00 |
| DP | 312.14 | 551.91 | 592.23 |

## 5. CONCLUSIONS

A multi-mode control strategy based on the driving pattern recognition scheme for hybrid electric truck was developed to minimize fuel consumption and engine-out emissions over various driving scenarios. Six representative driving patterns with defined characteristics were selected to represent different driving modes. For each representative driving pattern, Dynamic Programming technique was utilized to determine the optimal power split and gear shift trajectory. The implementable, sub-optimal control algorithm associated with each representative driving pattern is then extracted by analyzing those optimal control actions. This design methodology by learning from the Dynamic Programming (DP) results has the clear advantage of being near-optimal, accommodating multiple objectives, and systematic.

The driving pattern recognition algorithm was used to determine which representative driving pattern is closest to the current driving pattern and switch the current control algorithm to the corresponding one. It was found that this multi-mode control can be adapted to the different driving scenarios and achieve significant performance improvement in almost all the cycles we tested.

## ACKNOWLEDGEMENT

The work of Soonil Jeon and Jang Moo Lee at Seoul National University, Korea was supported in part by a grant from the BK-21 Program. The work of Chan-Chiao Lin and Huei Peng at the University of Michigan is supported by the U.S. Army TARDEC under the contract DAAE07-98-C-R-L008.

## REFERENCES

[1] Lin, C., Kang, J., Grizzle, J. W. and Peng, H., "Energy Management Strategy for a Parallel Hybrid Electric Truck," Proceedings of the 2001 American Control Conference, Arlington, VA, June, 2001, pp.2878-2883.

[2] Jeon, S. I., Jo, S. T., Park, Y. I., and Lee, J. M., "Multi - Mode Driving Control of a Parallel Hybrid Electric Vehicle Using Driving Pattern Recognition," Journal of Dynamic Systems, Measurement, and Control, ASME, March, 2002, Vol. 124, Issue 1, pp. 141~149.

[3] Bertsekas, D.P., Dynamic Programming and Optimal Control, Athena Scientific, 1995

[4] Lin, C., Kang, J., Grizzle, J. W. and Peng, H., "Power Management Strategy for a Parallel Hybrid Electric Truck," Proceedings of the 10th Mediterranean Conference on Control and Automation, Lisbon, Portugal, July 2002

[5] Kang, J., Kolmanovsky, I., and Grizzle, J. W., "Dynamic Optimization of Lean Burn Engine Aftertreatment," ASME Journal of Dynamic Systems, Measurement and Controls, Volume 123, Number 2, Page 153-160, June 2001

[6] National Renewable Energy Laboratory, USA, *Advanced Vehicle Simulator ADVISOR, ver 3.2,* 2001.